Dielectric tensor and collective modes in a two-dimensional electron liquid in a magnetic field

Kenneth I. Golden*
Department of Theoretical Physics, Research School of Physical Sciences and Engineering, The Australian National University, Canberra, Australian Capital Territory 2601, Australia

G. Kalman
Department of Physics, Boston College, Chestnut Hill, Massachusetts 02167

Philippe Wyns
Hewlett-Packard, Colorado Integrated Circuits Division, M.S. 64, 3404 East Harmony Road, Fort Collins, Colorado 80525
(Received 5 March 1993; revised manuscript received 10 May 1993)

This paper addresses the problem of collective-mode dispersion in the strongly coupled two-dimensional (2D) classical electron liquid in a perpendicular dc magnetic field. The system is modeled as a 2D one-component plasma sandwiched between two dielectric materials ε_1 and ε_2. For the strong-coupling regime $\bar{\Gamma} \equiv 2e^2/[(\varepsilon_1+\varepsilon_2)ak_BT] \gg 1$ (a is the 2D Wigner-Seitz radius), our analysis—which is carried out in the recently established quasilocalized-charge approximation [G. Kalman and K. I. Golden, Phys. Rev. A **41**, 5516 (1990)] with the input of the equilibrium pair-correlation function —indicates (i) that both magnetoplasmon and magnetoshear mode oscillations can be excited and (ii) that their dispersion is profoundly affected by the combined presence of strong particle correlations and the external magnetic field. The calculations cover the entire wave-number domain; typical dispersion curves are displayed for $\bar{\Gamma}=22$, 50, and 120. We make contact with well-established magnetoplasmon and magnetophonon dispersion calculations for the 2D Wigner crystal and with the magnetoplasmon dispersion of the uncorrelated 2D electron gas.

I. INTRODUCTION

There is a great deal of interest in the problem of collective-mode dispersion in two-dimensional (2D) electron systems in magnetic fields. Depending on the value of the coupling parameter determined by the ratio of the potential energy to the kinetic energy of the system ($\Gamma = e^2/ak_BT$ for a classical system, $r_s = a/a_B$ for a degenerate quantum system; a is the Wigner-Seitz radius and a_B is the Bohr radius), the system can be in the weakly correlated gaseous phase, strongly correlated liquid phase, or in the crystallized Wigner lattice state. The definitive treatment of the collective mode structure of the 2D degenerate electron gas in a magnetic field was given by Chiu and Quinn[1] in 1974; they calculated the magnetoplasmon oscillation frequency in the random-phase approximation (RPA). This was followed by the harmonic approximation calculations of Fukuyama[2] and Bonsall and Maradudin:[3] these investigators considered the 2D Wigner crystal in the quantum and classical domains and calculated the dispersion of the magnetoplasmon and magnetophonon excitations. The latter are the shear waves which propagate in solids. Going beyond the harmonic approximation, Côte and MacDonald[4] have recently calculated the collective-mode oscillation frequencies in the time-dependent Hartree-Fock approximation for the quantum 2D Wigner crystal in a strong magnetic field. Thus there is a reasonably good understanding at the present time of the collective-mode structure of the 2D magnetized electron system in the limiting cases of negligible and very strong coupling.

The mode structure in the domain of the strongly correlated liquid state, where most of the physically realizable systems occur, is much less understood. It is also here that the greatest differences between the behavior of the finite-temperature classical and the zero-temperature degenerate quantum system is expected. This paper addresses the problem of the magnetized 2D classical electron liquid: the calculation of the dielectric response tensor and collective-mode dispersion for such a system is the primary goal of the paper.

"Classical" 2D electron systems have been generated in the Grimes-Adams[5] and related[5] experiments, where the electrons are trapped on the surface of liquid He; in these situations the typical density ($n = 10^8$ cm^{-2}) and temperature ($T = 0.5$ K) values yield $\varepsilon_F/k_BT \ll 1$. The addition of a magnetic field does not affect the classical character of the system as long as the Landau level separation $\hbar\omega_c \ll k_BT$: for the temperature range quoted this allows $B_{0\max} \cong 3700$ Gs.

The model system we propose to study is the 2D one-component (electron) plasma (OCP) in a constant uniform magnetic field perpendicular to the plane of the plasma. For complete generality, we let the OCP monolayer be sandwiched between two dielectric materials ε_1 and ε_2. The strength of the particle-particle interactions in the 2D system is characterized by the coupling param-

0163-1829/93/48(12)/8882(8)/$06.00

eter $\overline{\Gamma}\equiv 2e^2/[a(\varepsilon_1+\varepsilon_2)k_BT]$, where a is the 2D Wigner-Seitz radius; $\pi a^2 n=1$. It is well established[5] that the system crystallizes into a triangular lattice at $\overline{\Gamma}_m=137\pm 15$.

The calculation of the dielectric response tensor will be carried out on the basis of the quasilocalized-charge (QLC) model which was introduced in Ref. 6 and employed in Refs. 7 and 8. Ample discussion of the justification, methodology, and limitations of the model have been given in Refs. 6, 8, and 9. The calculation based on the model provides the dielectric-response function and related quantities as functionals of the equilibrium pair-correlation function. The effect of the external magnetic field is easily incorporated in the formalism through the equation of motion; no modification of the magnetic-field-free pair-correlation function is necessary as long as the classical character of the system is maintained. Thus the Monte Carlo (MC) simulation[10,11] and hypernetted chain (HNC) calculation[11,12] data for the pair-correlation function used in our earlier works[7,8] can be employed here as well. The results of the calculations identify two modes, the magnetoplasmon and the magnetoshear modes, as the principal excitations of the magnetized 2D electron liquid. In this respect the liquid is similar to the Wigner solid, but in contrast to solids, liquids can sustain shear modes for finite wave numbers $k>k_{\min}$ only. Roughly speaking, this is the result of the competition between the characteristic time of the slow diffusion and migration of the particles from their quasiequilibrium positions and the oscillation period of the mode. Only when the former is longer than the latter can the collective oscillation be maintained. This should be kept in mind since the diffusion migration process is not described by the QLC model.

Molecular-dynamics (MD) simulations[13] of the magnetic-field-free 2D OCP confirm the existence of shear modes in the liquid phase for $\overline{\Gamma}>22$ and over a restricted wave-number domain. Our own recent calculations[8] indicate that the 2D classical electron liquid can indeed sustain shear waves at wavelengths sufficiently short to preclude the possibility of disruption of the mode by particle diffusion. Guided by these observations, we concentrate in the present paper on the $1\ll\overline{\Gamma}<\overline{\Gamma}_m$ liquid-phase domain where the "magnetoshear" mode is expected to occur.

In addition to the collective modes proper, which are confined to the 2D layer, one can also identify a "radiative mode"[14] which corresponds to an electromagnetic wave propagating in the surrounding dielectric medium (or vacuum) and being radiated out by the collective motion of the particles. Such a mode, strictly speaking, has no three-dimensional analog, since it requires a system occupying a bounded region in space; similar scenarios for finite three-dimensional slabs have, however, been discussed.[14]

The plan of the paper is as follows: In Sec. II we establish the QLC microscopic-equation-of-motion basis for the calculation of the linear response (to small external scalar and vector potential perturbations) and dynamical matrix. The calculation of the susceptibility and dielectric-response tensors follows in Sec. III. The results of Secs. II and III are applied in Sec. IV where we calculate the dispersion of the magnetoplasmon and magnetoshear modes. Conclusions are drawn in Sec. V.

II. EQUATION OF MOTION AND DYNAMICAL MATRIX

In this section we apply the QLC methodology of Refs. 6–9 to the system under consideration. We consider a monolayer sandwiched between two dielectric media and pervaded by a constant, uniform magnetic field as an OCP consisting of a 2D classical electron liquid immersed in a uniform neutralizing background of positive charge. The N electrons occupy the large but bounded area S in the plane $z=0$, of a Cartesian coordinate system; $n=N/S$ is the areal density. The two dielectric media are characterized by dielectric constants ε_1 ($z>0$ domain) and ε_2 ($z<0$ domain). The constant magnetic field $\mathbf{B}_0$ is applied in the direction normal to the plane of the OCP. The 2D OCP plasma frequency is given by $\omega_p(k)=\sqrt{2\pi ne^2k/m}$, where $-e$ and m are the electron charge and mass; the wave vector $\mathbf{k}$ lies in the plane $z=0$.

We wish to calculate the linear response to small perturbing scalar and vector potentials $\hat{\Phi}(\mathbf{k}\omega)$ and $\hat{\mathbf{A}}(\mathbf{k}\omega)$. Here $\hat{\mathbf{E}}(\mathbf{k}\omega)=(i\omega/c)\hat{\mathbf{A}}(\mathbf{k}\omega)-i\mathbf{k}\hat{\Phi}(\mathbf{k}\omega)$ is understood to be the external electric field acting at the interface of the two dielectric constant media in the absence of the plasma layer, but in the presence of the dielectric media.[15] As a preliminary step, we derive the expression for the dynamical matrix $\mathbf{C}(\mathbf{k}\omega)$ that controls the dynamics of the collective coordinates.[6,8,9] To this end, we consider the microscopic equations of motion describing the rapid oscillations of the charges about their slowly drifting quasiequilibrium site positions. Let $x_{i,\mu}$ be the quasiequilibrium site position of the ith charge and $\xi_{i,\mu}(t)$ the perturbed amplitude of its small excursion about $x_{i,\mu}$ (i and j enumerate particles and μ and ν are 2D vector indices; Einstein summation convention for repeated vector indices is understood). The microscopic equation of motion for the ith particle can now be written as follows:

$$-m\omega^2\xi_{i,\mu}(\omega)+\sum_j\{K_{ij,\mu\nu}(\omega)+M_{ij,\mu\nu}(\omega)\}\xi_{j,\nu}(\omega)$$
$$=im\omega\omega_c\eta_{\mu\nu z}\xi_{i,\nu}(\omega)-\frac{e}{S}\sum_{\mathbf{q}}\hat{E}_\mu(\mathbf{q}\omega)e^{i\mathbf{q}\cdot\mathbf{x}_i}\ ; \quad (1)$$

$\omega_c=eB_0/mc$ is the cyclotron frequency, $\eta_{\mu\nu\sigma}$ is the permutation pseudotensor. The $K_{ij}(\omega)$ term contains the effect of the longitudinal Coulomb interaction between the particles,

$$K_{ij,\mu\nu}(\omega)=\frac{1}{S}\sum_{q\geq\omega/c}q_\mu q_\nu\frac{\bar{\beta}(q\omega)}{q}\frac{\phi(q)}{\bar{\varepsilon}(q\omega)}$$
$$\times\{e^{i\mathbf{q}\cdot(\mathbf{x}_i-\mathbf{x}_j)}-\delta_{ij}e^{i\mathbf{q}\cdot\mathbf{x}_i}n_q+N\delta_{ij}\delta\mathbf{q}\}\ , \quad (2)$$

while the $\mathbf{M}_{ij}(\omega)$ term originates from the transverse retarded electromagnetic interparticle interaction,

$$M_{ij,\mu\nu}(\omega)=\frac{1}{S}\sum_{q\geq\omega/c}(q_\mu q_\nu-q^2\delta_{\mu\nu})\frac{\bar{\beta}(q\omega)}{q}\frac{\phi(q)}{(qc/\omega)^2-\bar{\varepsilon}(q\omega)}(1-\delta_{ij})e^{i\mathbf{q}\cdot(\mathbf{x}_i-\mathbf{x}_j)}\ . \tag{3}$$

The wave vector $\mathbf{q}$ lies in the plane $z=0$, $\phi(q)=2\pi e^2/q$ is the Fourier transform of the 2D Coulomb potential $\phi(r)=e^2/r$ (r is the distance in the plane $z=0$); the unperturbed ("base") microscopic density $n_{\mathbf{q}}=\sum_j e^{-i\mathbf{q}\cdot\mathbf{x}_j}$ depends on the $\mathbf{x}_j$ coordinates of the random sites. The appearance of

$$\bar{\beta}(q\omega)=\frac{2\beta_1(q\omega)\beta_2(q\omega)}{\beta_1(q\omega)+\beta_2(q\omega)}\ ,$$
$$\beta_m(q\omega)=\sqrt{q^2-(\varepsilon_m\omega^2/c^2)}\quad(m=1,2) \tag{4}$$

is a consequence of the required exponential decay[15] (with increasing distance from the $z=0$ plane) of all electromagnetic field quantities: it is the well-known feature of the 2D geometry that the $\beta_m^2>0$ condition guarantees this behavior.[1,3,16] The mean dielectric constant

$$\bar{\varepsilon}(q\omega)=\frac{\beta_1(q\omega)\varepsilon_2+\beta_2(q\omega)\varepsilon_1}{\beta_1(q\omega)+\beta_2(q\omega)} \tag{5}$$

portrays the presence of the dielectric materials.[15]

The calculation of the dynamical matrix $\mathbf{C}(\mathbf{k}\omega)$ from Eqs. (1)–(3) is carried out by further implementing the QLC procedure of Ref. 6. We obtain

$$C_{\mu\nu}(\mathbf{k}\omega)=\omega_p^2(k)\left\{L_{\mu\nu}(\mathbf{k})\frac{\bar{\beta}(k\omega)}{k\bar{\varepsilon}(k\omega)}-T_{\mu\nu}(\mathbf{k})\frac{\bar{\beta}(k\omega)}{k[(kc/\omega)^2-\bar{\varepsilon}(k\omega)]}+\bar{D}_{\mu\nu}(\mathbf{k}\omega)-\bar{Q}_{\mu\nu}(\mathbf{k}\omega)\right\}-i\omega\omega_c\eta_{\mu\nu z}\ . \tag{6}$$

$T_{\mu\nu}(\mathbf{q})=\delta_{\mu\nu}-q_\mu q_\nu/q^2$ and $L_{\mu\nu}(\mathbf{q})=q_\mu q_\nu/q^2$ are notationally convenient transverse (T) and longitudinal (L) projection tensors in the two-dimensional plane. The first two terms in (6) represent the effect of the average RPA field on the dynamics. The important correlation-induced Coulomb part of the dynamical matrix $\bar{\mathbf{D}}(\mathbf{k}\omega)$ (with both longitudinal and transverse elements) is

$$\bar{D}_{\mu\nu}(\mathbf{k}\omega)=\frac{1}{kS}\sum_{q\geq\omega/c}L_{\mu\nu}(\mathbf{q})\frac{\bar{\beta}(q\omega)}{\bar{\varepsilon}(q\omega)}\{g(|\mathbf{k}-\mathbf{q}|)-g(q)\} \tag{7}$$

where $g(|\mathbf{k}-\mathbf{q}|)$ and $g(q)$ are Fourier transforms of the equilibrium pair-correlation function. The correlation-induced electromagnetic part $\bar{\mathbf{Q}}(\mathbf{k}\omega)$ consists also of longitudinal and transverse contributions,

$$\bar{Q}_{\mu\nu}(\mathbf{k}\omega)=\frac{1}{kS}\sum_{q\geq\omega/c}T_{\mu\nu}(\mathbf{q})\frac{\bar{\beta}(q\omega)}{(qc/\omega)^2-\bar{\varepsilon}(q\omega)}g(|\mathbf{k}-\mathbf{q}|)\ . \tag{8}$$

Both the longitudinal and transverse elements of $\bar{\mathbf{Q}}(\mathbf{k}\omega)$ are, however, relativistically small and are therefore discarded in another paper of ours.[8]

The frequency dependence of $\bar{\mathbf{D}}(\mathbf{k}\omega)$ is a consequence of the $\bar{\beta}(q\omega)/\bar{\varepsilon}(q\omega)$ factor in Eq. (7). It is not difficult to show that, within the domain of nonrelativistic approximation, one can replace $\bar{\beta}(q\omega)$ by q, $\bar{\varepsilon}(q\omega)$ by $\bar{\varepsilon}\cong(\varepsilon_1+\varepsilon_2)/2$, and lift the restriction on the $\mathbf{q}$ summation. Thus $\bar{\mathbf{D}}$ becomes frequency independent and, not surprisingly, turns out to be the $\bar{\mathbf{D}}(\mathbf{k})$ of Ref. 8, screened by the substrate mean dielectric constant $\bar{\varepsilon}$. The knowledge of the dynamical matrix enables one to derive the dispersion relation for the collective modes. One obtains

$$\mathrm{Det}\{\omega^2\mathbf{I}-\mathbf{C}(\mathbf{k}\omega)\}=\left\{\omega^2-\omega_p^2(k)\left[\bar{D}_L(\mathbf{k})+\frac{\bar{\beta}(k\omega)}{k\bar{\varepsilon}(k\omega)}\right]\right\}\times\left\{\omega^2-\omega_p^2(k)\left[\bar{D}_T(\mathbf{k})-\frac{\bar{\beta}(k\omega)/k}{(kc/\omega)^2-\bar{\varepsilon}(k\omega)}\right]\right\}-\omega^2\omega_c^2=0\ . \tag{9}$$

III. SUSCEPTIBILITY AND DIELECTRIC RESPONSE TENSORS

More detailed information on the properties of the system can be gleaned by studying the susceptibility and surface dielectric response tensors.

In a recent publication,[15] a two-dimensional phenomenological electrodynamics has been worked out entirely in terms of field quantities defined inside the electron monolayer. Within this strictly 2D framework, the full surface dielectric-response tensor $\boldsymbol{\epsilon}(\mathbf{k}\omega)$ can be constructed in terms of the 2D *total* (or "screened") susceptibility tensor $\boldsymbol{\xi}(\mathbf{k}\omega)$ of the plasma monolayer and in terms of the surrounding dielectric media:[15]

$$\boldsymbol{\epsilon}(\mathbf{k}\omega)=\bar{\varepsilon}(\mathbf{k}\omega)\mathbf{I}+2\pi\bar{\beta}(k\omega)\boldsymbol{\xi}(\mathbf{k}\omega)\ . \tag{10}$$

$\boldsymbol{\xi}(\mathbf{k}\omega)$ portrays the response of the average first-order current density response $\mathbf{j}(\mathbf{k}\omega)$ to the *total* (external plus induced) electric-field perturbation.

The calculation of $\boldsymbol{\xi}(\mathbf{k}\omega)$ is carried out by deriving the QLC equation of motion for $\mathbf{j}(\mathbf{k}\omega)$ according to the procedure of Refs. 8 and 9 and comparing with the appropriate constitutive relation.[15] Choosing $\mathbf{k}=(0,k)$, we obtain

$$\boldsymbol{\xi}(\mathbf{k}\omega)=-\frac{ne^2}{m}\Delta^{-1}(\mathbf{k}\omega) \tag{11}$$

where

$$\Delta_{\mu\nu}(\mathbf{k}\omega)=\omega^2\delta_{\mu\nu}-\omega_p^2(k)\bar{D}_{\mu\nu}(\mathbf{k})+i\omega\omega_c\eta_{\mu\nu z}\ . \tag{12}$$

The eigenfrequencies $\omega(\mathbf{k})$ can then be determined from the dispersion relation

$$\mathrm{Det}\left\{\left[\frac{kc}{\omega}\right]^2 \mathsf{T}(\mathbf{k})-\epsilon(\mathbf{k}\omega)\right\}=0 \ . \tag{13}$$

IV. COLLECTIVE MODES

The unmagnetized 2D OCP can support two collective excitations.[1,8] The longitudinal plasmon mode[1,7] is maintained by the average field and, although modified by correlations, is already present in the weakly coupled gas. The transverse shear mode is induced by correlations and therefore it manifests itself in the strongly correlated liquid[8] or crystalline lattice[3] only. The presence of the external magnetic field does not alter this general scenario, though it strongly modifies the dispersion of the modes as shown both in the RPA calculation of the electron gas[17] and in the case of the Wigner lattice.[3] Here we derive the dispersion relation for the strongly coupled electron liquid and bridge the gap between the two extreme situations. Recent quantum-mechanical calculations for the strongly magnetized 2D electron liquid occupying the lowest Landau level only[4] have provided quite similar results.

In addition to the collective modes proper, which decay exponentially away from the layer, the magnetized 2D OCP can support—in contrast to the unmagnetized 2D OCP—a radiative mode which corresponds to an electromagnetic wave propagating in the surrounding dielectric medium and being radiated out by the collective motion of the particles.

Our calculations are based on the dispersion relation (13) or, equivalently, on the dispersion relation (9).

A. Magnetoplasmon mode

In a very good approximation (as discussed below) the quasistatic condition $kc \gg \omega$ can be adopted for both modes. In the domain of its validity, Eq. (9) simplifies to

$$\{\omega^2-\bar{\omega}_p^2(k)[1+D_L(\mathbf{k})]\}\cdot\{\omega^2-\bar{\omega}_p^2(k)D_T(\mathbf{k})\}=\omega_c^2\omega^2 \tag{14}$$

with the magnetoplasmon solution

$$\begin{aligned}\omega^2(\mathbf{k})=&\tfrac{1}{2}\{\bar{\omega}_p^2(k)[1+D_L(\mathbf{k})+D_T(\mathbf{k})]+\omega_c^2\}\\&+\tfrac{1}{2}(\{\bar{\omega}_p^2(k)[1+D_L(\mathbf{k})+D_T(\mathbf{k})]+\omega_c^2\}^2\\&-4\bar{\omega}_p^4(k)D_T(\mathbf{k})[1+D_L(\mathbf{k})])^{1/2} \ ;\end{aligned} \tag{15}$$

$\bar{\omega}_p^2(k)\equiv\omega_p^2(k)/\bar{\epsilon}$ and $\bar{\epsilon}\equiv(\epsilon_1+\epsilon_2)/2$. In the absence of particle correlations, $D_L=D_T=0$ and Eq. (38) reduces to the RPA expression $\omega^2(\mathbf{k})=\bar{\omega}_p^2(k)+\omega_c^2$ reported by Horing and Yildiz.[17]

To see in detail the effect of the strong particle-particle correlations on the magnetoplasmon dispersion, we consider first the long-wavelength domain $\omega_c a/c \ll ka \ll 1$. Equation (5) then further simplifies to

$$\omega^2(\mathbf{k})=\omega_c^2+\bar{\omega}_p^2(k)\left[1+D_L(\mathbf{k})+D_T(\mathbf{k})\frac{\omega_c^2}{\omega_c^2+\bar{\omega}_p^2(k)}\right] \tag{16}$$

where $D_L(\mathbf{k}\to 0)$ and $D_T(\mathbf{k}\to 0)$ are $O(k)$ terms and are to be expressed in terms of the correlation energy per particle (see Refs. 7 and 8). At $\bar{\Gamma}=\bar{\Gamma}_m=137\pm 15$, the 2D classical electron liquid freezes into a triangular lattice[5] and the total static ground-state energy per electron is $E_c(\bar{\Gamma}_m)=-1.1061e^2/a\bar{\epsilon}$.[3,18] When this is introduced as the correlation energy into (16) via Eqs. (17) and (18) of Ref. 8, the resulting expression for the long-wavelength magnetoplasmon oscillation frequency is in near-perfect numerical agreement with the Bonsall-Maradudin[3] result for the 2D hexagonal Wigner lattice.

Equation (16) has been cast in the form that clearly shows the difference between the correlation contributions to the (magneto)plasmon mode in the magnetized and unmagnetized situations. For $B_0=0$, the $O(k^2)$ contribution in Eq. (16) originates from $D_L(\mathbf{k})$ only, while for any $B_0\neq 0$, it is generated by the combined $D_L(\mathbf{k})+D_T(\mathbf{k})$ resulting in a maximum 20% drop in the coefficient of the k^2 terms in Eq. (16). This effect could provide a clear observable signature distinguishing the correlationally induced coefficient from those originating from other sources (finite layer width, impurities, etc.).

We have calculated $D_L(\mathbf{k})$ and $D_T(\mathbf{k})$ and then $\omega(\mathbf{k})$ from Eq. (15) using MC $g(r)$ data from Refs. 10 and 11 and HNC $g(r)$ calculations from Ref. 11. Some caution should be exercised, however, in using the HNC data for small k ($ka<1$) values, since the HNC results (without additional bridge diagram corrections) are quite unreliable in this domain. The resulting magnetoplasmon dispersion curves are displayed in Figs. 1 and 2 for $\bar{\Gamma}=22,50,120$ and $\omega_c/\bar{\omega}_0=0,0.1,1.0[\bar{\omega}_0=(2\pi e^2 n/ma\bar{\epsilon})^{1/2}]$. The zero-magnetic-field case (plasmon dispersion) has already been analyzed and discussed in some detail in Ref. 8. The magnetoplasmon dispersion, similarly to the plasmon dispersion,[8] develops a maximum and then exhibits oscillations which originate from the short-range order in the correlated liquid. As k increases beyond the long-wavelength domain described by Eq. (16), $\omega(\mathbf{k})$ increases to its maximum and thereafter descends through a series of oscillations to the asymptotic value

$$\omega(k\to\infty)=\omega_{\infty+}\equiv\tfrac{1}{2}\{\omega_c+\sqrt{\omega_c^2+4\omega_*^2}\} \ , \tag{17}$$

$$\begin{aligned}&\omega_*^2=\bar{\omega}_0^2 f(\bar{\Gamma}) \ ,\\&f(\bar{\Gamma})=-\frac{a}{4\pi}\int_0^\infty dq\, q^2 g(q) \ ,\\&f(\bar{\Gamma}>90)=0.411 \ .\end{aligned} \tag{18}$$

For a given $\bar{\Gamma}$ value, the oscillations become more and more suppressed as the applied magnetic field is increased. The asymptotic formula (17) is quite remarkable as it is completely different from the $k\to\infty$ RPA behavior [$\omega(k\to\infty)\to\infty$ in the "hydrodynamic" RPA description]. It is not difficult to show that $\omega_{\infty+}$ is pre-

cisely the higher of the two gyration frequencies of an isolated particle in a magnetic field surrounded by a disk of neutralizing background charge density, which for $\bar{\Gamma} > 90$ is not distinguishable from a uniformly distributed one: this provides the 0.411 coefficient in (18) [cf. a similar discussion in Ref. 8, Eq. (37)].

The polarization of the magnetoplasmon both at $k=0$ and at $k \to \infty$ is right circular, i.e., agreeing with the rotational sense of the electron in the magnetic field. For finite k values the polarization picks up a longitudinal component.

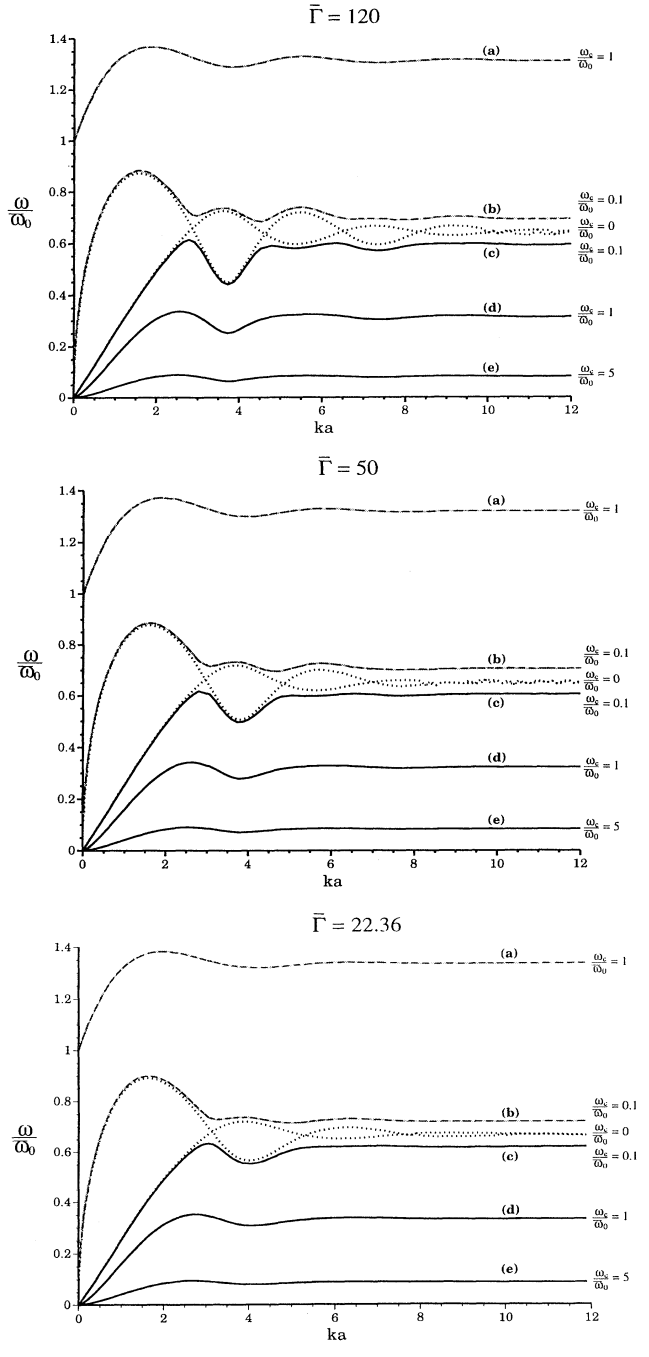

FIG. 1. Dispersion of the magnetoplasmon mode [curves (*a*) and (*b*)] and magnetoshear mode [curves (*c*), (*d*), and (*e*)] for $\bar{\Gamma}=22.36$, 50, and 120 calculated from Eqs. (14), (15), (38), and (52). The boundary longitudinal plasmon and transverse shear modes are also shown for zero magnetic field.

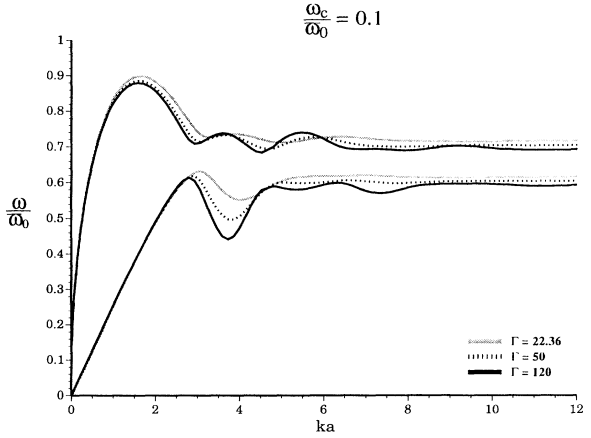

FIG. 2. Dispersion of the magnetoplasmon mode (upper three curves) and magnetoshear mode (lower three curves) for $\omega_c/\bar{\omega}_0=0.1$ and $\bar{\Gamma}=22.36$, 50, and 120 calculated from Eqs. (14), (15), (38), and (52).

In the strong-field limit, the magnetoplasmon oscillation frequency

$$\omega(\mathbf{k})=\omega_c+\frac{\bar{\omega}_p^2(k)}{2\omega_c}[1+D_L(\mathbf{k})+D_T(\mathbf{k})] \tag{19}$$

results from Eq. (15) for *all* $ka \gg \omega_c a/c$. This is identical to the long-wavelength result reported by Bonsall and Maradudin[3] and is also quoted as Eq. (36b) in Ref. 4.

The "strong-magnetic-field" limit should be understood with the condition $k_B T \gg \hbar\omega_c$ in mind, which ensures the classical behavior of the system. Thus, for both conditions to be satisfied $\hbar\omega_c$ has to be bracketed between $\hbar\omega_0$ and $k_B T$. In combination with the $\bar{\Gamma} \gg 1$ relation this sets an upper limit on the density, which is, however, not too severe: with $n < 3\times 10^8$ cm^{-2}, all the above-mentioned conditions can be simultaneously satisfied. However, on physical grounds, one should expect that in the opposite limit, $k_B T \ll \hbar\omega_c$, when only the lowest Landau level is occupied with a low filling factor but the temperature is above its melting value, exchange effects are negligible and our formalism still holds, with an important *caveat*, though: it would be unjustified to use the classical static (B-independent) pair-correlation function for the determination of $\mathbf{D}(\mathbf{k})$. Thus such a calculation would become feasible only when the correctly calculated or computed quantum pair-correlation function for the strongly magnetized, strongly coupled 2D electron liquid becomes available.

We complete the analysis of the magnetoplasmon mode by examining the domain $ka \ll \bar{k}a$, where the boundary

$$\bar{k}a=\frac{e^2}{amc^2\bar{\varepsilon}}\left\{1+\left[1+2\frac{amc^2\bar{\varepsilon}}{e^2}\left[\frac{\omega_c}{\bar{\omega}_0}\right]^2\right]^{1/2}\right\} \tag{20}$$

is determined by the intersection between the light

line $\omega=kc$ and the $ka<1$ nonretarded $(c\to\infty)$ magnetoplasmon dispersion curve generated from Eq. (15). Taking $\omega_c/\bar{\omega}_0=0.1\sim1$, we see that the domain is always very narrow since, for classical electrons trapped on the free surface of liquid helium, $\overline{ka}\approx(\omega_c/\omega_0)(2e^2/amc^2)^{1/2}=10^{-6}(\omega_c/\omega_0)n^{1/4}=(0.13-1.3)\times10^{-4}$ at a typical areal density $n=3\times10^8$ cm^{-2} realized in the Grimes-Adams experiment.[5] In this domain the physical requirement $\beta_1^2(k\omega)>0$, $\beta_2^2(k\omega)>0$ dictates that for $\varepsilon_1>\varepsilon_2$, $\omega\to kc/\sqrt{\bar{\varepsilon}_1}$ from below as $k\to0$. Consequently, $\beta_1(k\omega)\ll\beta_2(k\omega)\cong k\sqrt{1-\varepsilon_2/\varepsilon_1}$, $\bar{\beta}(k\omega)\approx2\beta_1(k\omega)$, and $\bar{\varepsilon}(k\omega)\approx\varepsilon_1$, resulting in the magnetoplasmon oscillation frequency

$$\omega(k\to0)=\frac{kc}{\sqrt{\bar{\varepsilon}_1}}\left\{1-2\left[\frac{ka}{\lambda_1\varepsilon_1}\right]^2+ka\left[\frac{8e^2}{amc^2}\right]\frac{\bar{D}_L(\mathbf{k}\to0)}{\varepsilon_1\lambda_1^2}\right\}, \tag{21}$$

$$\lambda_1\equiv\frac{8e^2}{amc^2\varepsilon_1}+\frac{\omega_c^2}{\omega_0^2},$$

with $\omega_0^2=2\pi ne^2/ma$. Equation (21) is reported here for the first time, but, except for the negligibly small correlation-induced correction proportional to $\bar{D}_L$, it amounts to a restatement of the light-line limit reported by Chiu and Quinn[1] and Bonsall and Maradudin[3] and is included primarily for the sake of completeness.

B. Magnetoshear mode

For the case where $\varepsilon_1=\varepsilon_2$, it can be rigorously demonstrated *a posteriori* [by numerically solving (9)] that the magnetoshear mode oscillation frequency $\omega(\mathbf{k})$ always satisfies the condition $kc\gg\omega(\mathbf{k})$. On physical grounds this condition should prevail for $\varepsilon_1\neq\varepsilon_2$ as well. Thus for the magnetoshear mode, $\beta_1(k\omega)\approx k$, $\beta_2(k\omega)\approx k$, $\bar{\varepsilon}(k\omega)\approx\bar{\varepsilon}\equiv(\varepsilon_1+\varepsilon_2)/2$, and Eq. (9) simplifies to

$$\{\omega^2-\bar{\omega}_p^2(k)[1+D_L(\mathbf{k})]\}\times\left\{\omega^2\left[1+\frac{\bar{\omega}_p^2(k)}{k^2c^2}\right]-\bar{\omega}_p^2(k)D_T(\mathbf{k})\right\}=\omega^2\omega_c^2 . \tag{22}$$

In calculating the shear mode oscillation frequency from (22), we consider the two domains $k^2c^2\ll\bar{\omega}_p^2(k)$ [i.e, $ka\ll2e^2/(amc^2\bar{\varepsilon})$] and $k^2c^2\gg\bar{\omega}_p^2(k)$ [i.e., $ka\gg2e^2/(amc^2\bar{\varepsilon})$].

In the $ka\ll2e^2/(amc^2\bar{\varepsilon})$ wave-number domain, which, as discussed above, is quite negligible, Eq. (22) further reduces to the magnetoshear mode oscillation frequency

$$\omega^2(\mathbf{k})\equiv\omega_-^2(k)=\frac{\bar{\omega}_p^4(k)}{\omega_c^2+\dfrac{\bar{\omega}_p^4(k)}{k^2c^2}}D_T(\mathbf{k}) . \tag{23}$$

When there is no applied magnetic field ($\omega_c=0$), Eq. (23) becomes identical to the $ka\ll2e^2/(amc^2)\bar{\varepsilon}$ shear mode result reported in Ref. 8. Both with and without magnetic field in the $k\to0$ limit, $\omega\sim k^{3/2}$, but the magnetic field reduces the phase velocity by a factor $(1+B_0^2a^3/4e^2/a)^{1/2}$. Equation (23) also reveals that the magnetoshear mode is suppressed by high magnetic fields. The calculation which follow show that this is, in fact, true for $ka\gg2e^2/(amc^2\bar{\varepsilon})$ as well.

For the domain of real interest $ka\gg2e^2/(amc^2\bar{\varepsilon})$, Eq. (22) reduces to Eq. (14) with magnetoshear mode solution

$$\omega^2(\mathbf{k})=\tfrac{1}{2}\{\bar{\omega}_p^2(k)[1+D_L(\mathbf{k})+D_T(\mathbf{k})]+\omega_c^2\}-\tfrac{1}{2}(\{\bar{\omega}_p^2(k)[1+D_L(\mathbf{k})+D_T(\mathbf{k})]+\omega_c^2\}^2-4\bar{\omega}_p^4(k)D_T(\mathbf{k})[1+D_L(\mathbf{k})])^{1/2} . \tag{24}$$

In the long-wavelength domain $2e^2/(amc^2\bar{\varepsilon})\ll ka\ll1$, Eq. (24) further simplifies to

$$\omega^2(\mathbf{k})=\frac{\bar{\omega}_p^4(k)D_T(\mathbf{k})}{\omega_c^2+\bar{\omega}_p^2(k)} \tag{25}$$

where $D_T(k\to0)$ is expressed in terms of the correlation energy.[8] Equation (24) and the correlation energy formulas quoted in Ref. 8 provide a complete description of long-wavelength magnetoshear mode dispersion in the classical 2D electron liquid. In the crystalline phase, substitution of the total ground-state energy per electron $E_c(\bar{\Gamma})=-1.1061e^2/a\bar{\varepsilon}$ into (25) via Eq. (18) of Ref. 8 results in a magnetoshear mode oscillation frequency which is in near-perfect numerical agreement with the Bonsall-Maradudin[3] low-k result for the 2D hexagonal Wigner-lattice.

Equation (25) is written again in the form that clearly shows the profound effect of the magnetic field on the dispersion of the magnetoshear mode. In the absence of a magnetic field $\omega(k\to0)$ has the acoustic, $\sim k$, behavior. In the presence of the magnetic field, however, $\omega(k\to0)\sim k^{3/2}$. This is in agreement with the behavior of the 2D Wigner lattice[3] and with the results of Ref. 4. Our numerical calculations of the magnetoshear mode frequency from (24) are displayed in Figs. 1 and 2, for $\bar{\Gamma}=22,50,120$ and $\omega_c/\bar{\omega}_0=0,0.1,1.0,5.0$. Oscillations in the magnetoshear mode dispersion, induced by the short-range order, set in at some point beyond the long-wavelength domain $ka<1$ described reasonably well by Eq. (25). As $k\to\infty$, the magnetoshear mode oscillation frequency reaches the asymptotic value

$$\omega(k\to\infty)=\omega_{\infty-}\equiv\tfrac{1}{2}\{\sqrt{\omega_c^2+4\omega_*^2}-\omega_c\} \tag{26}$$

where ω_*^2 is defined in (18). $\omega_{\infty-}$ is now the *lower* of the two gyration frequencies of an isolated particle in a magnetic field surrounded by a disk of neutralizing background charge density.

The polarization of the magnetoshear mode is transverse linear for $k\to0$, becoming elliptical for finite k, turning into left circular as $k\to\infty$.

The separation of the asymptotic limits of the magnetoplasmon and magnetoshear modes $\delta\omega_\infty=\omega_{\infty+}-\omega_{\infty-}=\omega_c$. Even though this is a correlational effect, once the correlations are strong enough, it becomes evidently independent of the coupling parameter and of the electron density. As such, this phenomenon

offers a characteristic, possibly observable, signature for the correlational dispersion.

The magnetoshear mode oscillation frequency becomes more and more suppressed with increasing magnetic field. In the strong-field limit (understood with the proviso stated in the discussion of the magnetoplasmon mode) the oscillation frequency

$$\omega(\mathbf{k})=\frac{\bar{\omega}_p^2(k)}{\omega_c}\sqrt{D_T(\mathbf{k})[1+D_L(\mathbf{k})]} \tag{27}$$

results from Eq. (24) for all $ka \gg 2e^2/(amc^2\bar{\epsilon})$. Both the $k\to 0$ and the strong-field limits are in agreement with the long-wavelength magnetophonon dispersion reported by Bonsall and Maradudin[3] and are also quoted in Ref. 4.

The zero-magnetic-field case ($\omega_c=0$) corresponding to the transverse shear mode has been extensively analyzed in Ref. 8.

No attempt has been made in this paper to analyze the damping of the two modes discussed, yet some inference can be drawn as to the expected features of the damping from our earlier studies of the longitudinal[7] and transverse[8] modes of the unmagnetized 2D electron liquid, based on the combined QLC mean-field theory approach. Both the longitudinal plasmon mode and the transverse shear mode undergo Landau damping in the large wave-number domain. The critical wave number beyond which the mode practically ceases to exist is a monotonically increasing function of Γ: for $\Gamma=50$ and 120 the respective maximum k values are $ak^{\rm pl}_{\rm max}(\Gamma=50)\cong 2.8$ and $ak^{\rm pl}_{\rm max}(\Gamma=120)\cong 3.5$ for the plasmon and $ak^{\rm shear}_{\rm max}(\Gamma=50)\cong 5.0$ and $ak^{\rm shear}_{\rm max}(\Gamma=120)\cong 8.0$ for the shear mode.

The magnetic field has a profound effect on the Landau damping mechanism. Since it inhibits the free motion of particles along the wave, only collision-assisted motion can result in the Landau damping required resonance between the particle velocity and the phase velocity of the wave. Thus one would expect a substantial reduction of the Landau damping for high wave numbers with a concomitant increase in the maximum k value. As a result, the observation of the high-k behavior of the dispersion (oscillatory approach to the asymptotic value), masked by Landau damping in the magnetic-field-free situation, may become observable.

A further effect of the magnetic field on the Landau damping mechanism is via the changed polarization of the waves. The appearance of a right-circular component in the polarization makes it possible for quasistationary electrons to resonate with the wave and to give rise to cyclotron damping when $\omega=\omega_c$. Only the magnetoplasmon mode has the right polarization to be a candidate for being affected by this mechanism: its frequency, however, always exceeds ω_c. Nevertheless, in the full kinetic treatment,[1] resonances with the ensuing cyclotron damping also develop at integer multiples of the cyclotron frequency,[19] $\omega=n\omega_c$. For weak enough magnetic field, damping in the vicinity of these harmonics may affect the magnetoplasmon; but for strong fields ($\omega_c \gtrsim \bar{\omega}_0/2$), as it is clear from the inspection of Figs 1 and 2 that, at most the second harmonic could come into play.

In addition to the high-k Landau damping, the magnetic-field-free shear mode is also damped at low-k values, and extinguished as $k\to 0$, by diffusional damping.[8] We have estimated[8] and inferred from MD data[13] $ak_{\rm min}(\Gamma=50)=0.64$ and $ak_{\rm min}(\Gamma=120)=0.21$. In the magnetized situation the magnetic field hinders the diffusion of the particles across the field: only collisions and electric-field fluctuations make it at all possible. Thus, similarly to the case of Landau damping, it is expected that the nonpropagating k region is diminished, with the $k_{\rm min}$ value being reduced, making it possible to observe low-k magnetoshear modes in the liquid phase.

C. Radiative mode

The interaction of the plasma layer with a propagating electromagnetic mode results in a radiative mode. Such a mode is characterized by complex values of $\beta(k\omega)=\sqrt{k^2-(\omega^2/c^2)}$ [cf. Eq. (4)] and of ω, for a real value of k. (We consider here only the $\epsilon_1=\epsilon_2=1$ situation.) Setting $\omega=\omega'+i\omega'', \beta=-i(q'+iq'')$, the choice of $\omega''<0$ entails $q''<0$, i.e., the wave $e^{-i(\omega t-qz)}$ decays in time, while it appears to grow in the z direction. To obtain the desired dispersion relation one looks for a solution of Eq. (9) satisfying $\omega'>kc, \omega''<0$. One finds for long wavelengths up to $O(k^4)$,

$$\omega=\omega_c\left\{1-d\frac{(ka)^2}{\omega_c^2+\omega_t^2}+\frac{1}{8}\frac{\omega_t^2}{\omega_c^2}\frac{3\omega_c^2-\omega_t^2}{(\omega_c^2+\omega_t^2)^3}(kc)^4\right\}$$
$$-i\omega_t\left\{1+d\frac{(ka)^2}{\omega_c^2+\omega_t^2}+\frac{1}{8}\frac{\omega_c^2-3\omega_t^2}{(\omega_c^2+\omega_t^2)^3}(kc)^4\right\} \tag{28}$$

where the coefficient d ($d>0$) originates from the small-k expansions of $D_L(\mathbf{k})$ and $D_T(\mathbf{k})$ [cf. Eqs. (17) and (18) of Ref. 8]:

$$d=-\frac{\omega_p^2(k)}{2(ka)^2}\{D_L(k\to 0)+D_T(k\to 0)\}$$
$$=-\frac{1}{8}\frac{\beta E_c(\Gamma)}{\Gamma}\omega_0^2\,. \tag{29}$$

The frequency

$$\omega_t=\frac{\omega_p^2(k)}{kc}=\frac{2\pi e^2 n}{mc} \tag{30}$$

is always much smaller than ω_c ($\omega_c/\omega_t=B_0a^2/2e$).

We see that only the magnetoplasmon gets converted into a radiative mode. The magnetoshear, because of its low phase velocity, does not couple to the electromagnetic radiation. The radiative mode describes a process through which energy is radiated out from the system. As a result, the mode is damped in time and appears to be growing in space (away from the plane), since the more distant position of the wave train was radiated out at an earlier epoch. The appearance of the radiative mode, by itself, is not a correlational effect: the $O(1)$ and $O(k^4)$

terms in (28) can be obtained from RPA calculations. In contrast, the leading k^2 dispersion comes entirely from correlations and is *negative* while the correlation independent k^4 dispersion is positive. Thus the measurement of the very long-wavelength dispersion in the radiative mode should provide another possible observational signature of the strong correlations in the 2D electron liquid. The $\omega' > kc$, i.e., $k < \omega_c/c$, condition means that the radiative mode survives only in the very-long-wavelength [$ka \leq 10^{-4}$; cf. the discussion following Eq. (20)] domain; but this is precisely the domain of interest from the point of view of probing the system through optical experiments.

V. CONCLUSIONS

In this paper we have calculated the dielectric-response tensor and collective-mode dispersion for a strongly coupled 2D classical electron liquid in a magnetic field. We have shown that the magnetoplasmon mode, already present in the uncorrelated electron gas,[1] is substantially modified by the strong electron-electron correlations. We have identified the magnetoshear mode, as a new excitation in the liquid state, maintained by strong particle correlations. We have also determined the existence of a radiative mode, characteristic to the magnetized situation, whose dispersion is governed largely by correlations.

In Secs. II and III, we calculated the dynamical matrix, and susceptibility and dielectric-response tensors in the quasilocalized charge approximation.[6] In Sec. IV we then calculated the dispersion of the magnetoplasmon and shear modes at strong coupling [$\bar{\Gamma} = e^2/(\bar{\varepsilon} a k_B T) \gg 1$] and over the entire wave-number domain. The resulting dispersion curves (Figs. 1 and 2) and the mode oscillation frequencies given by Eqs. (15), (16), (24), and (25) coupled with the Ref. 8 liquid state formulas for $D_L(\mathbf{k})$ and $D_T(\mathbf{k})$ show how the collective-mode dispersions are affected by particle correlations and the interplay between the latter and the applied magnetic field. Qualitatively this can be summarized as follows: (i) Both collective modes exhibit an oscillatory dispersion caused by short-range order. (ii) For $\omega_c/\bar{\omega}_0 \leq 0.1$, the oscillations become more pronounced with increasing $\bar{\Gamma}$; for $\omega_c/\bar{\omega}_0 > 1$, the dispersion is essentially unaffected as $\bar{\Gamma}$ increases beyond 50. (iii) For a given value of $\bar{\Gamma}$ the oscillations—and, indeed, the magnetoshear mode itself—become more and more suppressed as $\omega_c/\bar{\omega}_0$ is increased. (iv) There is a qualitative difference in the coefficient determining the slope of the magnetoplasmon dispersion curve [Eq. (16)] as compared with the coefficient of the slope of the ordinary plasmon, even for very weak magnetic fields. (v) For high-k values ($k \to \infty$) the magnetoplasmon and the magnetoshear frequencies approach $\omega_{\infty+}$ and $\omega_{\infty-}$, respectively, the gyration frequencies of an isolated charge in a neutralizing 2D background; the $\omega_{\infty+} - \omega_{\infty-}$ separation is always ω_c, irrespective of the values of the other parameters of the system. (vi) The polarization of the magnetoplasmon is right-circular both for $k \to 0$ and for $k \to \infty$; it picks up a longitudinal component for intermediate k values. The polarization of the magnetoshear mode is transverse linear for $k \to 0$, changing into left circular as k increases. (vii) We expect that both Landau and diffusional dampings of both of the modes are substantially lower than those of their magnetic-field-free counterparts. As to the radiative mode, its main features are that (i) its frequency is in the vicinity of ω_c; (ii) it is weakly damped, with a damping of the order ω_t; and (iii) its dominant k^2 dispersion is determined entirely by the correlation energy of the system (should, however, one include thermal dispersion in the formulation of the dielectric function, other, kinetic-energy-related k^2 contributions would probably also occur).

It is hoped that the theoretical predictions of this paper will motivate both molecular-dynamics simulations for the magnetized 2D OCP and new laboratory experiments on 2D electron monolayers on the surface of liquid helium, with the addition of a constant magnetic field normal to the surface.

ACKNOWLEDGMENTS

This work has been partially supported by the National Science Foundation Grants Nos. PHY-9115695, PHY-9115714, and INT-9215300. One of us (K.I.G.) wishes to thank the Department of Theoretical Physics, RSPhysSE, Institute of Advanced Studies, The Australian National University for hospitality.

*Permanent address: Department of Computer Science and Electrical Engineering, The University of Vermont, Burlington, VT 05405.

[1] K. W. Chiu and J. J. Quinn, Phys. Rev. B **9**, 4724 (1974).
[2] H. Fukuyama, Solid State Commun. **17**, 1323 (1975).
[3] L. Bonsall and A. A. Maradudin, Phys. Rev. B **15**, 1959 (1977).
[4] R. Côte and A. H. MacDonald, Phys. Rev. B **44**, 8759 (1991).
[5] C. C. Grimes and G. Adams, Phys. Rev. Lett. **42**, 795 (1979). A. J. Dahm and W. F. Vinen, Phys. Today, **40** (2), 43 (1988).
[6] G. Kalman and K. I. Golden, Phys. Rev. A **41**, 5516 (1990).
[7] K. I. Golden, G. Kalman, and Ph. Wyns, Phys. Rev. A **41**, 6940 (1990).
[8] K. I. Golden, G. Kalman, and Ph. Wyns, Phys. Rev. A **46**, 3463 (1992).
[9] K. I. Golden, G. Kalman, and Ph. Wyns, Phys. Rev. A **46**, 3454 (1992).
[10] H. Totsuji, Phys. Rev. A **17**, 399 (1978).
[11] R. C Gann, S. Chakravarty, and G. V. Chester, Phys. Rev. B **20**, 326 (1979).
[12] F. Lado, Phys. Rev. B **17**, 2827 (1978).
[13] H. Totsuji and N. Kakeya, Phys. Rev. A **22**, 1220 (1980).
[14] Ronald Fuchs, K. L. Kliewer, and W. J Pardee, Phys. Rev. **150**, 589 (1966); K. L. Kliewer and R. Fuchs, *ibid.* **144**, 495 (1966); **150**, 573 (1966).
[15] See K. I. Golden and G. Kalman, Phys. Rev. B **45**, 5834 (1992).
[16] A. L. Fetter, Ann. Phys. (N.Y.) **81**, 367 (1973).
[17] N. J. Horing and M. Yildiz, Phys. Lett. A **44**, 386 (1973).
[18] M. J. Lea and N. H. March, J. Phys. Condens. Matter **3**, 3493 (1991).
[19] I. Bernstein, Phys. Rev. **109**, 10 (1958).